Eur Biophys J (2007) 36:337–347
DOI 10.1007/s00249-007-0135-5

ARTICLE

Stability and fusion of lipid layers on polyelectrolyte multilayer supports studied by colloidal force spectroscopy

Guido Köhler · Sergio E. Moya · Stefano Leporatti · Christian Bitterlich · Edwin Donath

Received: 26 September 2006 / Revised: 11 January 2007 / Accepted: 17 January 2007 / Published online: 9 February 2007

Abstract The interaction between lipid layers supported by polyelectrolyte multilayer cushions has been studied by means of colloidal force spectroscopy. In a typical experiment, a colloidal probe engineered with a layer-by-layer film and a lipid bilayer on top is approached to a planar surface coated in a symmetrical way. Kinks of a few nanometres in width appear when lipid layers are pressed together—reflecting either fusion processes between lipid layers or membranes, or the penetration of polymer blobs into or through the lipid layers. Retracting curves show a stepwise shape, which results from lipid tether formation or from polymer stretching, the latter suggesting that polyelectrolyte multilayers make contact as a result of penetration or lipid fusion.

Keywords Atomic force · Surface engineering · Nanocomposites · Lipid–polyelectrolyte interactions

Dedicated to Prof. K. Arnold on the occasion of his 65th birthday.

G. Köhler (✉) · S. Leporatti · C. Bitterlich · E. Donath
Institute of Medical Physics and Biophysics, Medical Faculty, University of Leipzig, Härtelstraße 16–18, 04107 Leipzig, Germany
e-mail: guido.koehler@medizin.uni-leipzig.de

S. E. Moya
CiCbiomagune, Paseo Miramón 182, 20009 San Sebastian, Gipuzkoa, Spain

S. Leporatti
National Nanotechnology Laboratory of CNR-INFM, Via Arnesano, 73100 Lecce, Italy

Abbreviations

AFS	Atomic force spectroscopy
CFS	Colloidal force spectroscopy
DMPA	1,2-Dimyristoyl-phosphatidic acid
DMPC	1,2-Dimyristoyl-phophatidylcholine
DOPC	1,2-Dioleoyl-phosphatidylcholine
LBL	Layer-by-layer technique
PAH	Poly(allylamine hydrochloride) Mw 70,000
POPC	1-Palmitoyl-2-oleoyl-phosphatidylcholine
PS	Polystyrene
PSS	Poly[(styrene sulfonate) sodium salt] Mw 70,000
SFM	Scanning force microscopy

Introduction

The design and fabrication of biomimetic colloids has become an important area in materials science research. Biomimetic colloids have recently attracted interest, for example, in the fields of drug delivery and diagnostics. It is quite a challenging task to design biocompatible particles as carriers with proper size and stability and also additional features, such as a targeting site and the possibility of controlled delivery. Different concepts for drug delivery devices have been explored to meet these requirements. Liposomes (Andresen et al. 2005; Sun and Chiu 2005), nanoparticles (Kickhoefer et al. 2005; Oh et al. 2005), colloids (Pichot 2004), dendrimers (Jang and Kataoka 2005; Pantos et al. 2005), polymeric vesicles (Soga et al. 2005; Bellomo et al. 2004), and polyelectrolyte multilayer capsules (Donath et al. 1998, 2002) have been widely studied regarding their potential for controlled

delivery and targeting. Each approach has its own benefits and disadvantages.

Our own research has focused on the engineering of colloids by means of depositing polyelectrolyte multilayers applying the layer-by-layer technique (LBL) and the subsequent fabrication of polyelectrolyte capsules as potential carrier systems (Decher 1997; Donath et al. 1998, 2002; Moya et al. 2000, 2003; Georgieva et al. 2000; Fischlechner et al. 2005). The LBL technique with its stepwise deposition protocol allows various functions to be added to the system in an independent manner. The top layer, for example, can be designed to a large extent independently from the composition of the layers underneath.

A convenient way to provide biocompatibility to polyelectrolyte multilayer systems is to add a lipid layer on top of the polyelectrolyte cushion (Sackmann 1996; Moya et al. 2000; Fischlechner et al. 2005). Such a design mimics the structure of the cell surface. The polyelectrolyte multilayer plays the role of the cytoskeleton and the lipid layer behaves as an analogue of the phospholipid membrane of the cell. A lipid layer would provide the basis for the subsequent attachment of lipid membrane associated biological functions, e.g. viruses, receptors, proteins, avoiding at the same time unspecific interactions between biopolymers and the polyelectrolyte support.

Compared to lipid layers supported by solid substrates, which have been extensively studied (Tamm and McConnell 1985; Helm et al. 1989; Benz et al. 2004), lipid membranes on top of polyelectrolyte cushions are less tightly adsorbed and, therefore, better resemble the properties of biological membranes in terms of structure and dynamics. On the other hand, this might lead to lower stability. The proper characterisation of the assembled lipid layers and their structural behaviour when interacting with other colloids or surfaces is particularly important for the fabrication of lipid-virus composites for sensing (Fischlechner et al. 2006) or for the use of lipids as components in the fabrication of capsules for drug delivery (Moya et al. 2000). One of the relevant phenomena is the fusion of two approaching lipid membranes. The activation pressure for hemi fusion—a probable precursor of fusion—of softly supported bilayers is considerably smaller than for rigidly supported bilayers (Seitz et al. 2001).

In this work, we have studied by means of colloidal force spectroscopy (CFS) the interaction of two lipid layers, each supported by polyelectrolyte multilayers. In a typical experiment, a colloidal probe engineered with an LBL film with a lipid layer on top is approached to a planar surface bearing a symmetrical composition. The different phenomena observed during the approach and retraction of the colloidal probe are described and characterised, such as discontinuities (''kinks'') in the force versus separation curves, and the adhesion between the two opposite lipid layers after pressing them together. Special emphasis is given to understanding how the structure and composition of the assemblies can influence the stability and fusion phenomena exhibited by the lipid layers.

Experimental

Chemicals

Polymers

Poly(allylamine hydrochloride) Mw 70,000 (PAH) and poly[(styrene sulfonate) sodium salt] Mw 70,000 (PSS) were purchased from Sigma-Aldrich.

Thiols

3-Mercapto-1-propanesulfonic acid sodium salt was purchased from Sigma-Aldrich. 2-Amino-ethanethiol hydrochloride was obtained from Acros Organics.

Lipids

1,2-Dimyristoyl-phosphatidylcholine (DMPC), 1,2-dioleoyl-phosphatidylcholine (DOPC), 1-palmitoyl-2-oleoyl-phosphatidylcholine (POPC), 1,2-dimyristoyl-phosphatidic acid (DMPA), and cholesterol were purchased from Avanti Polar Lipids.

Polystyrene (PS) latex particles of 20.8 μm diameter were obtained from Microparticles GmbH, Berlin, Germany.

Polyelectrolyte coating

All substrates were coated with polyelectrolytes by means of the LBL deposition technique (Sukhorukov et al. 1998) by dipping them with an alternating protocol into solutions of 1 g/l PAH or PSS, respectively, in the presence of 0.5 M NaCl. Between coating steps, non-adhered polyelectrolytes were washed away with 0.1 M NaCl.

Onto PS latex particles, five or nine single layers were assembled in order to obtain a positively charged top layer. Glass planar substrates were first cleaned following standard RCA cleaning procedures (Itano et al. 1993) and then coated in the same way as the colloidal sphere until the desired number of layers and charge were achieved.

Thiol adsorption

Gold-coated slides (Arrandee) were first flame-annealed and then modified with a thiol self-assembled monolayer to obtain a charged surface (Bain et al. 1989). The thiols were adsorbed overnight from a 5 mM solution in ethanol, followed by rinsing with ethanol and water.

Lipid coating

Phospholipid vesicles were prepared by dissolving lipids in a chloroform solution, which was afterwards evaporated in a rotavap. The lipids were then re-dispersed in water by 20 min sonication to obtain small unilamellar vesicles. The final lipid concentration was 1 mg/ml. The coating of the polyelectrolyte or thiol coated substrates and colloids was performed by adding the lipid vesicle solution. The vesicles were left in contact with the respective substrate for 10 min, unless otherwise noted. After incubation, the substrates were washed several times with distilled water (Georgieva et al. 2000; Fery et al. 2003; Troutier et al. 2005; Correia et al. 2004). It must be underlined that the adsorption of vesicles onto the probing latex sphere was performed when the latter had already been glued to the cantilever used for force measurements (see below). This was done to prevent contact of the lipids with air and to avoid defects on the lipid membrane during handling.

Force measurements

CFS, atomic force spectroscopy (AFS), and scanning force microscopy (SFM) were conducted using the Molecular Force Probe (MFP) 1D and 3D instruments (Asylum Research, Santa Barbara, CA, USA). The MFP has an open fluid cell design and was used in combination with an inverted optical microscope, Olympus IX 70 (1D) or IX 71 (3D), equipped with a 40× objective.

CSC12/Tipless/No Al cantilevers from MikroMasch (Tallinn, Estonia) were used for the CFS studies. A PS latex particle was glued with epoxy resin (UHU Plus Endfest 300, Uhu GmbH, Bühl, Germany) to the tipless cantilever before the coating. MSCT-AUHW cantilevers from Veeco Instruments (Woodbury, NY, USA) were used for the AFS and SFM measurements in which no colloidal probes were employed. The spring constant was determined for each cantilever separately using the thermal noise method.

All measurements were carried out in Millipore water at 24.5 ± 0.5°C with a driving velocity of 1 μm/s. When the reproducibility became worse (due to the manifold interaction cycles, which finally resulted in the destruction of the composite build-up (Butt 1991; Ducker et al. 1991; Bosio et al. 2004; Leporatti et al. 2005)), care was taken to stop the acquisition of force versus distance curves. Images of lipid surfaces were recorded in tapping mode because of the possible damage of the samples in contact mode by even relatively low forces.

Results and discussion

The SFM micrographs in Fig. 1 show the topology of an LBL film composed of $(PAH/PSS)_2PAH$ (Fig. 1a) and the changes that take place in the surface after coating the film with lipid layers consisting of DMPC (Fig. 1b) or DMPC/cholesterol (70:30) (Fig. 1c), respectively. The surface of the polyelectrolyte multilayer shows a few grains on quite a smooth plane. These grains or patches are up to 15 nm high and up to some 100 nm wide, which is consistent with previous findings (Moya et al. 2003; Leporatti et al. 2000). The root-mean-squared roughness of the surface is 3.6 nm (calculated after zeroth-order flattening). After coating with DMPC, the grains appear a bit more pronounced, while most of the surface retains the roughness of the LBL layers (overall roughness 5.5 nm). The expanded

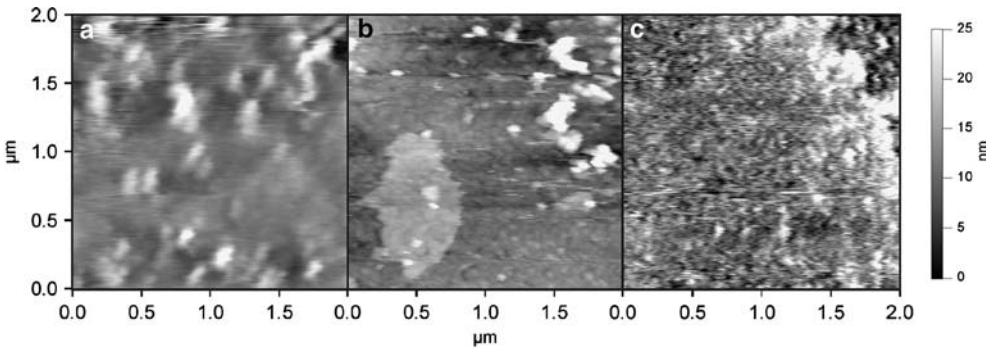

Fig. 1 SFM images of a glass surface coated with **a** $(PAH/PSS)_2PAH$ in contact mode, **b** $(PAH/PSS)_2PAH$ + DMPC in tapping mode, and **c** $(PAH/PSS)_2PAH$ + DMPC/cholesterol (70:30) in tapping mode

patch of about 6 nm height in the bottom left corner of Fig. 1b is probably a second lipid layer or flattened, non-fused vesicles. The whole surface is covered by phospholipids as shown by AFS measurements, carried out with the same Si_3N_4 tip that was used for imaging (not shown). Coating polyelectrolyte multilayers with a mixture of DMPC/cholesterol (70:30) results in a more grainy texture (overall roughness 8.1 nm), but again the lipid coating is complete all over the scanned surface. The large elevation in the right-hand side of the micrograph is due to the roughness of the glass surface, likely caused by irregularities in the substrate already present before coating with the polyelectrolytes. The coating with POPC results in the best surface coverage. For this phospholipid, the roughness of the polyelectrolyte film is nearly retained after the lipid coating (4.4 nm, image not shown).

Figure 2 shows a typical force versus distance curve of a colloidal probe coated with polyelectrolytes and phospholipids interacting with a symmetrical surface. Upon approach of the two polyelectrolyte-supported lipid bilayers, kinks in the force curve can be seen, typically at loads of 1–10 nN. A kink is caused by a jump or a sudden displacement in the movement of the cantilever towards the interface. Kinks are not always present in force versus distance curves, but they appear for many of the investigated zwitterionic phospholipids. The width of the kink is estimated from the horizontal distance between the cusp and the increasing branch of the force versus distance curve. The histogram in Fig. 3 illustrates the distribution of the kink width for DMPC. The majority of kinks range from 2 to 6 nm in width, but kinks up to 16 nm can be observed as well. Even though kinks are not always present in the force versus distance curves, sometimes more than one kink can be observed. The frequency of occurrence of kinks is shown in the inset of Fig. 3. For example, for DMPC, the majority of the curves do not exhibit any kinks, but some experiments reveal two or even more kinks. The statistical analysis of the data shows that the frequency of occurrence of kinks follows a Poisson distribution, indicating that the number of kinks appearing in an experiment is a random variable. For POPC (data not shown), the kinks have a maximum width of 5 nm, most of them lying between 2 and 4 nm. Most of the force curves show at least one kink, while more than two kinks in a single curve have not been detected. A similar behaviour has been observed for a mixture of zwitterionic phospholipids with cholesterol, DMPC/cholesterol (70:30).

The question arises as to what could be the nature of these kinks. If the lipid layers fuse upon the external pressure applied during the approach, the cantilever will experience a sudden jump (model I, Fig. 4a). A lipid bilayer has a thickness of approximately 5 nm. Complete fusion would thus yield a kink width of 10 nm. Hemi fusion would result, instead, in 5 nm kink width. Such fusion events have been demonstrated for DMPC bilayers on polyethyleneimine by Wong et al. (1999). Because of the roughness and other topological constrains of the polyelectrolyte support, kinks with widths below 5 nm and above 10 nm could be expected.

Another explanation may be that kinks are caused solely by the roughness of the polymer multilayers

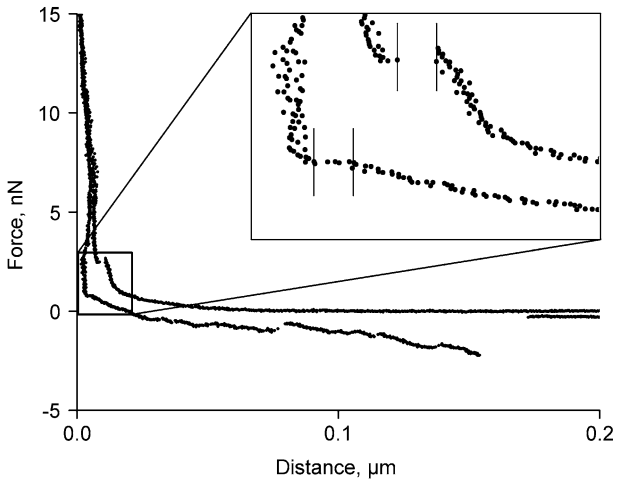

Fig. 2 Example of a force versus distance curve of a colloidal probe coated with $(PAH/PSS)_4PAH$ + POPC interacting with a glass surface coated in a symmetrical way. The occurrence of a kink is *highlighted* in the *curve*

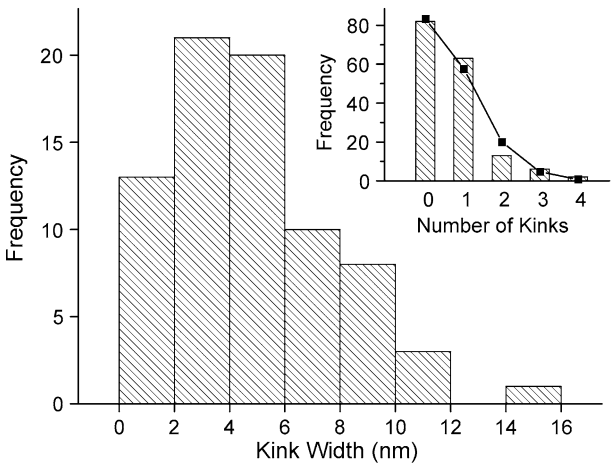

Fig. 3 Histogram showing the frequency of occurrence of kinks with a defined length during experiments performed with DMPC-modified colloidal probe. *Inset* histogram showing frequency of occurrence of a number of kink events in a single force versus distance experiment for the same experiments with DMPC. The curve is fitted with a Poisson distribution

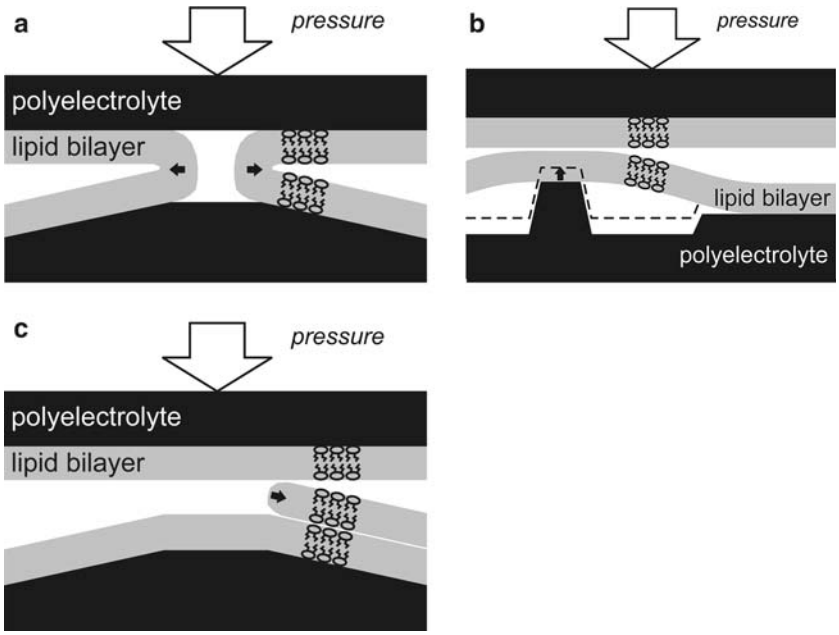

Fig. 4 Schemes of possible mechanisms of kink formation through **a** vesicle fusion (model I), **b** topological effects (model II), **c** dislocation of lipid layers (model III). For details of the three models see text

underneath. When pressing, polyelectrolyte patches may be forced through or into the lipid layers (model II, Fig. 4b). In this situation, the distance between the two interfaces will suddenly decrease according to the depth of polymer protrusion into the lipid layer(s). The width of most of the kinks (1–10 nm) is consistent with the mean roughness of the polyelectrolyte multilayers. The presence of more than one kink could also be explained—on this basis—as the penetration of the lipid layers in different areas. Richter and Brisson et al. (2003, 2006) reported similar kinks when performing force versus distances curves with a Si_3N_4 cantilever against supported membranes on different substrates. The jumps in their curves did not exceed 9 nm and were assumed to reflect the topology of the employed substrates as a result of pressing the membrane onto them. This explanation is similar to model II described above.

One could also assume that the lipid coverage is not homogeneous. For example, there could be patches of a second lipid layer adsorbed to the first layer, which could be the result of an incompletely spread vesicle. If so, the kinks could also be attributed to sudden lateral dislocations of these patches upon the applied load (model III, Fig. 4c). This hypothesis would be consistent with most of the observed kink widths.

To check whether a second lipid layer could form, the assembly of lipid vesicles on top of polyelectrolyte multilayer cushions was monitored in real time by means of quartz crystal microbalance with dissipation. The changes in frequency and dissipation upon DMPA or DMPC vesicle adsorption were studied, respectively (see Fig. 6 in Moya and Toca-Herrera 2006). Changes in frequency are related to the mass assembled on the surface, whereas the dissipation is related to the capability of the system to relax its mechanical energy and depends on the viscoelastic nature of a material. It is interesting to note that for DMPA the frequency reaches a plateau approximately 20 min after adding the vesicle solution. The dissipation keeps an almost constant value during the whole assembly. For DMPC, the situation is quite different. The coating of DMPC proceeds at the beginning significantly slower than for DMPA, without reaching a plateau. The frequency decreased continuously during the 15 h that the process was monitored. The dissipation increased over 600 min, approaching a final value of about 100, while the dissipation for DMPA never reached values above five. Modelling the data with the algorithms developed by Voinova et al. (1999), a thickness of 5 nm was calculated for the DMPA layer, while for DMPC the estimated thickness was about 15 nm. This is consistent with the ongoing formation of double or multiple layers over the time when the surface is in contact with a reservoir of lipid vesicles in the force microscopy measurements. It is worth mentioning that the very large dissipation observed during the DMPC assembly suggests the presence of adsorbed vesicles on the surface. A lipid bilayer coating the surface would behave like a solid structure and show a small dissipation like that exhibited by the DMPA bilayer.

The following considerations may help to differentiate among the three models. While in model I and eventually in model II (probably for larger kink

widths) the two polyelectrolyte supports will get into contact, in model III they will not. This situation should be reflected in the force retraction curves. Therefore, we compared the retracting curves of the lipid samples to those shown by the bare polyelectrolyte supports, where—in the absence of lipids—two polyelectrolyte multilayers are approached and retracted.

In many cases, for example, for POPC and DMPC, with or without cholesterol, the force curves show adhesion upon retraction, but this phenomenon is followed by a reasonably complex picture of rupture events. In the retraction curves in Fig. 5 one can observe the different characteristic events that take place. Indeed, retraction curves can be classified as (1) rupture sequences showing a sawtooth-like appearance. In a random fashion, a non-linearly increasing piecewise adhesion force is followed by rupture instabilities until finally the contact is lost. (2) Rupture traces with well-defined plateaus of constant adhesion forces upon retraction. These plateaus may extend over 100–400 nm. (3) Rupture traces where both features can be identified. Looking more carefully at the force curves recorded in quick succession at a particular position of a sample, we found that in general the first curves show plateaus of constant adhesion before the sawtooth-like shapes appeared.

In the absence of lipids (Fig. 6), the approaching curves show repulsion, as it would be expected from the fact that in the considered example both the sphere and the planar surface are coated with a last layer of positively charged PAH. Nevertheless, upon retraction adhesion with a sawtooth shape is almost always

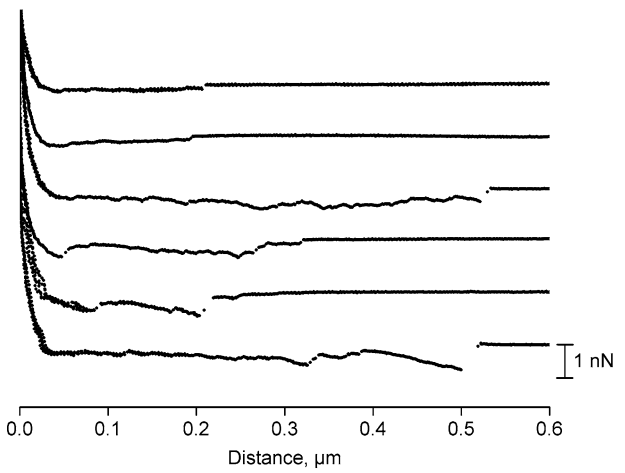

Fig. 5 Examples of retracting regions of force versus distance curves of colloidal probes coated with $(PAH/PSS)_4PAH$ + DMPC interacting with a glass surface coated in a symmetrical way

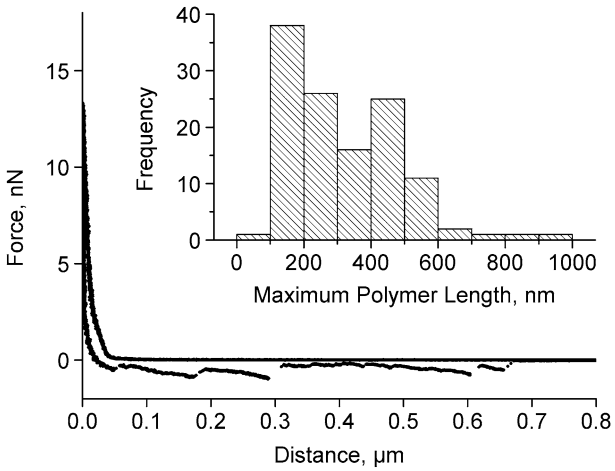

Fig. 6 Example of a force versus distance curve of a colloidal probe coated with $(PAH/PSS)_4PAH$ interacting with a glass surface coated in a symmetrical way. *Inset* histogram showing the frequency of appearance of events of polymer stretching of a defined length

observed. Sawtooth-like rupture events are generally considered to be caused by polymer stretching (Bustamante et al. 1994). This can be explained by an incomplete coverage of the polyelectrolyte layers. Molecular contact will then occur between the PAH on one surface and the oppositely charged PSS located underneath the PAH on the other surface. Polyelectrolyte molecules from both surfaces may remain electrostatically attached to the opposite surface and may anchor the colloidal probe while pulling away. With increasing separation, the polymers are stretched. This causes a nonlinear elastic response of the macromolecules provided by the entropic restoring force. The loss of contact occurs in a sequence of rupture events when more than one macromolecule chain spans the gap. It must be kept in mind that the colloidal probe arrangement provides a considerable contact area, given the large radius of the probing sphere. The distances at which the polymers rupture have a broad distribution (inset of Fig. 6). The polyelectrolyte chains are not necessarily attached with their end groups. In addition, the topology of the contact area provides a distribution of separation distances. The maximum chain length of PAH, Mw 70,000, can be calculated as 230 nm, considering the Mw of the monomer (93.56) and the C–C binding length (153 pm). The maximum length of PSS, also Mw 70,000, corresponds to 105 nm. Compared to these values, the distribution of the rupture lengths has maxima roughly at the respective chain lengths and at values that can be interpreted to result from two or more chains alternately sticking together, which are drawn from their respective layers.

From the similarity of the retraction forces, we can conclude for the samples coated with lipids that in many cases the polyelectrolytes underneath the lipid layers come into contact as result of the applied pressure. Thus, model III is less likely for the studied systems. However, it cannot be ruled out in cases where a force curve shows multiple kinks. The first kinks could be related to dislocation of lipid patches, while the last ones could reflect the fusion of two lipid layers or the perforation of a lipid layer by polyelectrolyte protrusions.

To gain more insights into the role of the polyelectrolytes, we have also studied supported membranes that lack the polyelectrolyte layers by AFS. Gold-coated glass substrates were covered by short chain thiols bearing either a positive or a negative charge at their end group. A lipid bilayer was subsequently deposited on top of the thiol monolayer following the same procedures as with the polyelectrolyte multilayers.

Typical force curves measured with a Si_3N_4 tip at the end of a cantilever are shown in Fig. 7. Conceptually, these experiments are very different from those described before. In the first place, the cantilever presents a nonsymmetrical configuration, with the lipids only present on the planar surface. Certain significant differences between the AFS and CFS experiments can be established. (1) Retracting forces are much lower due to the smaller contact area (tip radius is only about 10 nm). (2) Approaching curves lack the soft region

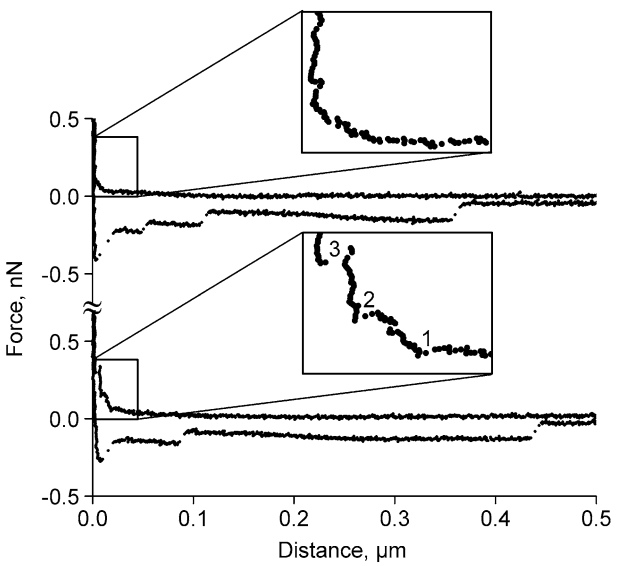

Fig. 7 Examples of force versus distance curves of a bare cantilever interacting with a gold surface coated with a negatively charged thiol + DOPC. Both curves have been obtained from the same sample

(about 10–30 nm wide) originated by the compressibility of the polyelectrolyte layers (Seitz et al. 2001) and the fuzzy surface of the PS latex used as colloidal probe. The origin of this region was confirmed in separate measurements with the naked PS latex against glass (data not shown). On the other hand, there are also similarities between the colloidal probe and the bare cantilever experiments. (1) Force curves with up to three kinks appear. (2) Ruptures are accompanied by plateaus of nearly constant adhesion. Remarkably, these adhesion forces have the same magnitude (about 100 pN) as those measured in the CFS experiments.

The occurrence of kinks in the AFS experiments is limited to samples, where the substrates had been in contact with the lipid suspension for a number of hours. With samples incubated only for 10–20 min, kinks are rarely detected. The experiments with the bare cantilever show another remarkable feature in the approach curves associated with the presence of kinks. Before the tip comes close to the surface of the solid substrate, it goes through a soft region of about 30–40 nm in height, which can be compressed or indented before finally hitting the solid substrate. Such a behaviour is not consistent with the idea of a homogeneously lipid-covered thiol/gold surface. It rather indicates the presence of incompletely spread lipid vesicles or lipid patches, which are first compressed by the tip and later eventually laterally dislocated or punctured (1st and 2nd kinks), or which get (hemi) fused by the tip (leftmost kink, bottom graph, Fig. 7).

Plateaus of constant force on retraction are known to be caused either by chain pulling or by a so-called lipid tether. The first hypothesis would mean that a macromolecule lying flat on a surface is gradually lifted. This might be relevant in the CFS but not in the AFS experiments. The second one implies that a tube-like cylindrical lipid bilayer is formed connecting the two interacting surfaces. Tether formation from cell-size capsules is a ubiquitous phenomenon (Evans and Yeung 1994). The extension of a tether requires a continuous flow of lipids into the forming tether, while the separation between two interacting surfaces is increasing. It could also be that a multilayer tube of lipids is thinning upon separation. Both ideas are consistent with a plateau of constant force reflecting resistance against flow and the work spent on the formation of a bent lipid surface.

The results of the AFS experiments allow two conclusions to be drawn: (1) since no polymers were present, the observed regions of constant forces in the retraction curves can only be explained by lipid tether pulling. Remarkably, the observed force is of the same order as that observed in the colloidal force set-up.

This is a strong argument for lipid tether pulling being the cause of the observed plateaus in both set-ups. (2) Since the kinks have been observed in correlation with imperfect lipid coating, it is quite likely that similar kinks observed in the colloidal force set-up can also be related to an irregular lipid coverage. A prolonged exposition of the thiol surfaces to the phospholipid vesicles could result in the formation of lipid multilayers or the further deposition of vesicles on top of the first assembled membranes. The tip could displace further membranes over the first membrane more easily than a membrane directly assembled on the thiol, since the interaction with the substrate (in this case another phospholipid membrane) will be weaker. If new vesicles assemble on top of an existing membrane, they may not form a perfect coating on the surface, but will rather leave free spaces and could be displaced more easily.

From the experiments with the bare tip at the end of the cantilever, we can estimate the applied pressure thanks to the fairly well-known geometry of the contact. A tip radius of 10 nm represents a mean contact area of about 140 nm^2. For this area, the measured force at the point of the kink (typically 0.15 nN) corresponds to a pressure of roughly 1 MPa. This value agrees with the one found for hemi fusion of DMPC bilayers by Seitz et al. (2001). Taking into account that kinks only occur in systems exhibiting imperfect lipid coating, it seems likely that we see hemi fusion at least in some cases of pronounced kinks. We do not assume a full fusion because of the necessary pressure of 5–10 MPa (Wong et al. 1999).

Similar kinks occurring on pressing a cantilever tip against a lipid layer adhered onto a mica support have been reported earlier (Butt and Franz 2002; Loi et al. 2002). The authors provide two alternative quantitative models for the initiation of a breakthrough. First, the continuum nucleation theory considers thermal fluctuations within the lipid layer and the energy of temporary holes. In this model, the free parameters are the spreading pressure and the line tension of the lipid layer. We obtained very low values of the spreading pressure as well as line tension (e.g. 0.58 mN/m and 2.61 pN, respectively, in the case of DOPC pressed by the cantilever tip). Second, the molecular model assumes jumps of the lipid molecules between certain binding sites that are energetically favourable positions. To jump from the initial position into an adjacent free position, a potential energy barrier has to be overcome. In the absence of the tip, adjacent binding sites are energetically equivalent. When the tip is pressed onto the film, a pressure gradient is applied, which increases the energy of the molecules. The probability of the occurrence of a breakthrough depends on the applied force, the tip radius, the rate of spontaneous hole formation, and the activated volume. Our data could be fitted by hole-formation rates of the order of 10 Hz, which again reflects the very weak binding of zwitterionic lipids. The data of the CFS experiments could not be satisfactorily fitted. The probable reasons are (1) that because of the size of the colloid and the roughness of the polyelectrolyte layers, the radii of the indenters are very heterogeneous, (2) neither the indenter nor the substrate is a really solid object, but they both show a rather elastic behaviour that influences the measured forces.

Assuming for the CFS experiments the same pressure of 1 MPa as in the bare tip experiment, the measured forces (1–10 nN) would correspond to contact area diameters of 36–113 nm. Interestingly, this range agrees well with the size of polyelectrolyte patches, which are 30–100 nm wide (Moya et al. 2003; Leporatti et al. 2000). It cannot be excluded that when this load is applied to a single polyelectrolyte grain sticking out from the interface, the grain is squeezed through the adsorbed lipid layer.

The electric charges at the edge of such a polyelectrolyte patch have to overcome the Born energy when coming into contact with the hydrophobic interior of the lipid layer. The Born energy for one ion of the polymer can be estimated as 2.8×10^{-19} J (assuming an ion radius of 0.2 nm, an ion charge of 1, and a dielectric constant for the lipid of 2). The whole energy applied by the load can be roughly estimated as the work that is done during the jump of the probing sphere. For typical values of 5 nN and 5 nm, respectively, this work is 2.5×10^{-17} J. Certainly, we overestimate the Born energy since the ions will not be completely surrounded by lipid, but rather only the outer ions of a patch will touch the lipids at only one side. Typically, the number of outer ions of a polyelectrolyte patch will be around 10^2, and for such a concentration of ions, the calculated work will be sufficient to push the patch through the lipid layer.

The squeezing of polyelectrolyte through lipid layers must be accompanied by a displacement of lipid molecules. One can imagine that they either could be moved within the plane of the lipid layer or out of plane. The latter is conceivable when the thickness of the polyelectrolyte patch is not too small or when there is free space resulting from an equally rough shape of the opposite surface due to polyelectrolyte granularity or incomplete coverage in the polyelectrolyte layers. For a displacement out of plane of lipids, the bending of the lipid layer is required. The bending energy can be calculated as

$$W_b = B/2 \int (1/R_1^{2+1/} R_2^{2)}\, dS$$

with B bending stiffness, R_1 and R_2 principal curvature radii, and S membrane surface (Canham 1970). Assuming $B \approx 1 \times 10^{-19}$ J (Méléard et al. 1997 and cit. therein), $R_1 = 5$ nm, and R_2 the radius of the polyelectrolyte patch, a bending energy in the order of 0.3–1×10^{-17} J can be estimated. This value is lower than the applied work. An energy consideration, however, is not capable of distinguishing between squeezing through and hemi fusion since also with the latter a similar membrane bending can be expected. In the case of hemi fusion, the polyelectrolyte patches may behave as a stamp defining the geometrical dimension of the detected event.

Moving lipid molecules within the plane of the lipid layer will be affected by the friction between the lipid head groups and the polyelectrolytes. We can observe the contribution of the adhesion when analysing the forces related to the pulling of lipid tethers. The pulling force F, which is required to form a lipid cylinder of radius R is given by $F = 2\,\pi\,B\,/\,R$ (Waugh and Hochmuth 1987). A lipid tether of 30 nm radius, which is a typical value for phosphatidylcholines (Evans and Yeung 1994), would thus require a force of about 10 pN. This value is too small to explain the observed pulling forces of circa 100 pN. Indeed, one has to take into account that in our case the lipid molecules are removed from a supported layer, rather than from a free membrane. Another contribution results from friction between the two halves of a bilayer at the bending site (Evans and Yeung 1994). These influences result in a considerable extra force. The jumps, which produced kinks in the force curves, consumed a time of 3 ± 1.5 µs. We can compare tether pulling and lipid displacement if we suppose that the necessary force is proportional to the number of involved lipid molecules per time unit. Provided the lipid comes from the adhered layer in both cases, which is likely because of the occurrence of polyelectrolyte contacts, the lateral displacement in-plane would need roughly a force of 60–900 nN. This exceeds the measured forces by 1–2 orders of magnitude and can, therefore, be excluded.

Obviously, a displacement of the lipids induced upon contact seems to be necessary for the oppositely charged polyelectrolyte species of both lipid coated interfaces to get into contact. Clearly it is also possible that the original lipid coverage was incomplete and some regions of the polyelectrolyte multilayer might have not been covered. These regions may be quite small and thus difficult to detect. For example, lipid patches not fused together after adsorption may be sufficient to establish contact between supporting polyelectrolyte cushions upon the applied load. It is also conceivable that the fusion between the lipid layer on the glass support and that on the probing sphere takes place upon the applied pressure. This would lead to the contact of the supporting multilayers.

The comparison of the different lipids used for coating suggests that the physicochemical properties of the lipid molecules play an important role for the degree of layer stability. Among these properties are head group charge, chain order, phase state, and in the case of mixtures also miscibility. These parameters will influence the binding strength between the lipids and the support as well as the intermolecular forces within the lipid layer. For example, the orientational order parameter of POPC is roughly twothird that of DMPC (Shin and Freed 1989). This may be related to the finding that the probability of kinks is higher for POPC compared to DMPC. The presence of cholesterol brings about manifold effects on phospholipid membranes. Miscibility phase separation tendencies are intrinsic to natural lipid/cholesterol mixtures (Rozovsky et al. 2005). Compared to cholesterol-free membranes, cholesterol lowers the lipid lateral diffusion (Almeida et al. 1992), enhances the bending modulus (Méléard et al. 1997), enlarges the area compression modulus (Evans and Needham 1986), and increases the vesicle rupture tension (ibid.). On the other hand, cholesterol shifted the PEG 6000 concentration necessary to induce phospholipid mixing of PC liposomes to lower concentrations, i.e. lower osmotic pressure (Zschörnig and Ohki 1993). In spite of the known stabilising and fusogenic effects, we saw only marginal influence on the frequency and critical forces of kinks. This might be an additional hint for the role of membrane defects for at least part of the observed kinks. An increased bending stiffness should hamper the formation of a closed lipid layer at the edges of polyelectrolyte patches during the lipid coating via adhered vesicles.

Indeed, little is known about how the polyelectrolyte support modifies the structure and dynamics of lipid layers compared to free membranes. In the case of a DMPC bilayer adsorbed to a PEI cushion, the aqueous compartment provided by the water-swollen polyelectrolyte cushion allows the lipid membrane to exist in a nearly unperturbed natural state (Seitz et al. 2001). This could be the case also with our system because the PEI molecules contain amino groups and, therefore, have a similar charge like the PAH used in this study. Another effect has been reported for polylysine adsorbed to DPPC/DPPA mixed liposomes.

In the range of 10–30% PA, the main transition splits into two transitions. This has been interpreted as a phase separation induced by different affinities of the lipid species to polylysine (Raudino et al. 1990). The charged moiety of polylysine is an amino group as well. We can only speculate whether this effect holds for our PC/cholesterol mixed bilayers leading to broad occurrence of areas of low or absent cholesterol, not distinguishable from pure PC samples.

Conclusion

We have presented a CFS study of the interaction between a colloidal probe modified with a lipid layer and a lipid layer deposited on a planar surface in a symmetrical situation, both supported by polyelectrolyte multilayers. While approaching both surfaces, discontinuities in the force versus distance curves are often observed. These discontinuities or kinks have a distribution of widths, which suggests either (hemi or full) fusion of the two opposing lipid layers or the perforation of one or both lipid layers by polyelectrolyte grains sticking out from the support. While full fusion can be excluded because of the insufficient forces, it is hard to come to a decision between hemi fusion and perforation. AFS experiments with only one lipid layer on the planar substrate and the bare tip yielded kinks. In this situation, the kinks that are induced by very weak forces may reflect dislocation of lipid patches (surplus layers). In various cases, the lipids of the opposite layers already get into contact on the action of relatively weak forces. In those cases, after repeated approach the samples end up with contact between the underlying polyelectrolytes, reflecting a local damage of the lipid layers. Retracting curves also show characteristic features: plateaus or sawtooth shapes, which are associated with the formation of lipid tethers and the pulling of polyelectrolyte molecules form the LBL film, respectively.

Colloidal force spectroscopy has been shown here to provide valuable information concerning the stability of lipid layers on colloidal particles. The choice of a proper lipid composition may be crucial for the fabrication of a biointerface on polymer capsules or colloids, where additional functions, e.g. viruses, receptors, proteins, will be assembled.

Acknowledgments The work was supported by grants from the German Federal Ministry for Education and Research (BMBF 0312011C) within the bionanotechnology programme and from the Volkswagenstiftung within the ''Complex Materials'' programme. Sergio Moya is a Ramon y Cajal fellow and thanks are due to the Ramon y Cajal programme for the support.

References

Almeida PFF, Vaz WLC, Thompson TE (1992) Lateral diffusion in the liquid phases of dimyristoylphosphatidylcholine/cholesterol lipid bilayers: a free volume analysis. Biochemistry 31:6739–6747

Andresen TL, Jensen SS, Jørgensen K (2005) Advanced strategies in liposomal cancer therapy: problems and prospects of active and tumor specific drug release. Prog Lipid Res 44:68–97

Bain CD, Troughton EB, Tao YT, Evall J, Whitesides GM, Nuzzo RG (1989) Formation of monolayer films by the spontaneous assembly of organic thiols from solution onto gold. J Am Chem Soc 111:321–335

Bellomo EG, Wyrsta MD, Pakstis L, Pochan DJ, Deming TJ (2004) Stimuli-responsive polypeptide vesicles by conformation-specific assembly. Nature Mater 3:244–248

Benz M, Gutsmann T, Chen N, Tadmor R, Israelachvili J (2004) Correlation of AFM and SFA measurements concerning the stability of supported lipid bilayers. Biophys J 86:870–879

Bosio V, Dubreuil F, Bogdanovic G, Fery A (2004) Interactions between silica surfaces coated by polyelectrolyte multilayers in aquaeus environment. Coll Surf A 243:147–155

Bustamante C, Marko JF, Siggia ED, Smith S (1994) Entropic elasticity of lambda-phage DNA. Science 265:1599–1600

Butt HJ (1991) Measuring electrostatic, van der Waals, and hydration forces in electrolyte solutions with an atomic force microscope. Biophys J 60:1438–1444

Butt HJ, Franz V (2002) Rupture of molecular thin films observed in atomic force microscopy. I. Theory. Phys Rev E 66:031601

Canham PB (1970) The minimum energy of bending as a possible explanation of the biconcave shape of the human red blood cell. J Theor Biol 26:61–81

Correia FM, Petri DFS, Carmona-Ribeiro AM (2004) Colloid stability of lipid/polyelectrolyte decorated latex. Langmuir 20:9535–9540

Decher G (1997) Fuzzy nanoassemblies: toward layered polymeric multicomposites. Science 277:1232–1237

Donath E, Sukhorukov GB, Caruso F, Davis SA, Möhwald H (1998) Novel hollow polymer shells by colloid-templated assembly of polyelectrolytes. Angew Chem Int Ed 37:2201–2205

Donath E, Moya S, Neu B, Sukhorukov GB, Georgieva R, Voigt A, Bäumler H, Kiesewetter H, Möhwald H (2002) Hollow polymer shells from biological templates: fabrication and potential applications. Chem Eur J 8:5481–5485

Ducker WA, Senden TJ, Pashley RM (1991) Direct measurement of colloidal forces using an atomic force microscope. Nature 353:239–241

Evans E, Needham D (1986) Giant vesicle bilayers composed of mixtures of lipids, cholesterol and polypeptides. Faraday Discuss Chem Soc 81:267–280

Evans E, Yeung A (1994) Hidden dynamics in rapid changes of bilayer shape. Chem Phys Lipids 73:39–56

Fery A, Moya S, Puech PH, Brochard-Wyart F, Mohwald H (2003) Interaction of polyelectrolyte coated beads with phospholipid vesicles. C R Physique 4:259–264

Fischlechner M, Zschörnig O, Hofmann J, Donath E (2005) Engineering virus functionalities on colloidal polyelectrolyte lipid composites. Angew Chem Int Ed 44:2892–2895

Fischlechner M, Toellner L, Messner P, Grabherr R, Donath E (2006) Virus-engineered colloidal particles—a surface display system. Angew Chem Int Ed 45:784–789

Georgieva R, Moya S, Leporatti S, Neu B, Bäumler H, Reichle C, Donath E, Möhwald H (2000) Conductance and

capacitance of polyelectrolyte and lipid–polyelectrolyte composite capsules as measured by electrorotation. Langmuir 16:7075–7081

Helm CA, Israelachvili JN, McGuiggan PM (1989) Molecular mechanisms and forces involved in the adhesion and fusion of amphiphilic bilayers. Science 246:919–922

Itano M, Kern FW Jr, Miyashita M, Ohmi T (1993) Particle removal from silicon wafer surface in wet cleaning process. IEEE Trans Semicond Manuf 6:258-267

Jang WD, Kataoka K (2005) Bioinspired applications of functional dendrimers. J Drug Del Sci Tech 15:19–30

Kickhoefer VA, Garcia Y, Mikyas Y, Johansson E, Zhou JC, Raval-Fernandes S, Minoofar P, Zink JI, Dunn B, Stewart PL, Rome LH (2005) Engineering of vault nanocapsules with enzymatic and fluorescent properties. Proc Natl Acad Sci USA 102:4348–4352

Leporatti S, Voigt A, Mitlöhner R, Sukhorukov GB, Donath E, Möhwald H (2000) Scanning force microscopy investigation of polyelectrolyte nano- and microcapsule wall texture. Langmuir 16:4059–4063

Leporatti S, Sczech R, Riegler H, Bruzzano S, Storsberg J, Loth F, Jaeger W, Laschewsky A, Eichhorn S, Donath E (2005) Interaction forces between cellulose microspheres and ultrathin cellulose films monitored by colloidal probe microscopy—effect of wet strength agents. J Colloid Interface Sci 281:101–111

Loi S, Sun G, Franz V, Butt HJ (2002) Rupture of molecular thin films observed in atomic force microscopy II. Experiment. Phys Rev E 66:031602

Méléard P, Gerbeaud C, Pott T, Fernandez-Puente L, Bivas I, Mitov MD, Dufourcq J, Bothorel P (1997) Bending elasticities of model membranes: influences of temperature and sterol content. Biophys J 72:2616–2629

Moya SE, Toca-Herrera JL (2006) From hollow shells to artificial cells: biointerface engineering on polyelectrolyte capsules. J Nanosci Nanotechnol 6:2329–2337

Moya S, Donath E, Sukhorukov GB, Auch M, Bäumler H, Lichtenfeld H, Möhwald H (2000) Lipid coating on polyelectrolyte surface modified colloidal particles and polyelectrolyte capsules. Macromolecules 33:4538–4544

Moya S, Richter W, Leporatti S, Bäumler H, Donath E (2003) Freeze-fracture electron microscopy of lipid membranes on colloidal polyelectrolyte multilayer coated supports. Biomacromolecules 4:808–814

Oh KS, Lee KE, Han SS, Cho SH, Kim D, Yuk SH (2005) Formation of core/shell nanoparticles with a lipid core and their application as a drug delivery system. Biomacromolecules 6:1062–1067

Pantos A, Tsiourvas D, Nounesis G, Paleos CM (2005) Interaction of functional dendrimers with multilamellar liposomes: design of a model system for studying drug delivery. Langmuir 21:7483–7490

Pichot C (2004) Surface-functionalized latexes for biotechnological applications. Curr Opin Colloid Interface Sci 9:213–221

Raudino A, Castelli F, Gurrieri S (1990) Polymer-induced lateral phase separation in mixed lipid membranes: a theoretical model and calorimetric investigation. J Phys Chem 94:1526–1535

Richter RP, Brisson A (2003) Characterization of lipid bilayers and protein assemblies supported on rough surfaces by atomic force microscopy. Langmuir 19:1632–1640

Richter RP, Bérat R, Brisson AR (2006) Formation of solid-supported lipid bilayers: an integrated view. Langmuir 22:3497–3505

Rozovsky S, Kaizuka Y, Groves JT (2005) Formation and spatio-temporal evolution of periodic structures in lipid bilayers. J Am Chem Soc 127:36–37

Sackmann E (1996) Supported membranes: scientific and practical applications. Science 271:43–48

Seitz M, Park CK, Wong JY, Israelachvili JN (2001) Long-range interaction forces between polymer-supported lipid bilayer membranes. Langmuir 17:4616–4626

Shin YK, Freed JH (1989) Thermodynamics of phosphatidylcholine–cholesterol mixed model membranes in the liquid crystalline state studied by the orientational order parameter. Biophys J 56:1093–1100

Soga O, van Nostrum CF, Fens M, Rijcken CJF, Schiffelers RM, Storm G, Hennink WE (2005) Thermosensitive and biodegradable polymeric micelles for paclitaxel delivery. J Control Release 103:341–353

Sukhorukov GB, Donath E, Lichtenfeld H, Knippel E, Knippel M, Budde A, Möhwald H (1998) Layer-by-layer self assembly of polyelectrolytes on colloidal particles. Coll Surf A 137:253–266

Sun BY, Chiu DT (2005) Determination of the encapsulation efficiency of individual vesicles using single-vesicle photolysis and confocal single-molecule detection. Anal Chem 77:2770–2776

Tamm LK, McConnell HM (1985) Supported phospholipid bilayers. Biophys J 47:105–113

Troutier AL Delair T, Pichot C, Ladavière C (2005) Physicochemical and interfacial investigation of lipid/polymer particle assemblies. Langmuir 21:1305–1313

Voinova MV, Rodahl M, Jonson M, Kasemo B (1999) Viscoelastic acoustic response of layered polymer films at fluid–solid interfaces: continuum mechanics approach. Physica Scripta 59:391–396

Waugh RE, Hochmuth RM (1987) Mechanical equilibrium of thick, hollow, liquid membrane cylinders. Biophys J 52:391–400

Wong JY, Park CK, Seitz M, Israelachvili J (1999) Polymer-cushioned bilayers. II. An investigation of interaction forces and fusion using the surface force apparatus. Biophys J 77:1458–1468

Zschörnig O, Ohki S (1993) Effect of cholesterol, diacylglycerol and phosphatidylethanolamine on PEG 6000 induced lipid mixing and surface dielectric constant of phosphatidylcholine vesicle. Gen Physiol Biophys 12:259–269